Synthesis of Higher Soluble Nanostructured Polyaniline by Vapor-Phase Polymerization and Determination of its Crystal Structure

Sambhu Bhadra, Joong Hee Lee

BIN Fusion Research Team, Department of Polymer and Nano Engineering, Chonbuk National University, Jeonbuk 561-756, South Korea

Received 16 December 2008; accepted 31 March 2009
DOI 10.1002/app.30524
Published online 2 June 2009 in Wiley InterScience (www.interscience.wiley.com).

ABSTRACT: Higher soluble nanostructured polyaniline was prepared by vapor-phase polymerization after passing aniline vapor through an aqueous acidic solution of ammonium persulfate (PANI-V). Polyaniline was also synthesized by the conventional oxidative polymerization method (PANI-C) in an aqueous medium for the comparison of its properties with PANI-V. PANI-V exhibited lower conductivity but higher hydrophilicity and higher solubility (2–3 times) in different solvents, such as tetrahydrofuran, *N*-methyl-2-pyrrolidone, dimethylsulfoxide, *N*,*N*-dimethyl formamide, and *m*-cresol at room temperature compared with that of PANI-C. The thermal stability of PANI-V was higher than that of PANI-C. In-depth investigations of the crystal structures of PANI-C and PANI-V were performed through powder X-ray diffraction analysis. The PANI-V showed a less ordered structure with a lower crystallinity and crystallite size and with a higher d-spacing and interchain separation compared with PANI-C. The unit cell volume of PANI-V was significantly higher with a greater number of atoms in the unit cell than that of PANI-C. © 2009 Wiley Periodicals, Inc. J Appl Polym Sci 114: 331–340, 2009

Key words: conjugated polymers; x-ray; crystal structures; FTIR

INTRODUCTION

Polyaniline (PANI) has attracted great attention because of its low-cost monomer, ease of synthesis, good thermal stability, tunable properties, and immense application possibilities.[1–7] However, the solubility of conventionally synthesized PANI is very low in most of the available solvents, rendering its effective application problematic. Attempts have been made to improve the solubility of PANI through doping with a suitable dopant or modifying the starting monomer.[6,8] Dopant significantly increases the conductivity of PANI, but the increase in solubility is not significant.[8] When aniline containing different substitution is polymerized, the resulting substituted PANI shows a higher solubility, though the conductivity decreases to a large extent compared with unsubstituted PANI.[9–11] For nanostructure materials, the surface area to volume ratio is very high, which has several significant implications.[12] Nanostructured PANI has several advantages for fabricating nano-devices.[13] Nanostructured PAni (nanofibers/nanotubes/nanowires/nanorods) have been prepared by electrospining,[14] hard templates,[15] soft templates,[16] interfacial polymerization,[17] dilute polymerization,[18] seeding polymerization,[19] etc. The present research is based on the vapor-phase polymerization of aniline to obtain a higher soluble nanostructured PANI. The main advantage of this method is the generation of simultaneously higher soluble and nanostructured PANI with good electrical conductivity. Understanding of the crystal structure for a semi-crystalline polymer, such as PANI, is very important for predicting its various properties, such as melting point, solubility, stability, and morphology.[20] However, few detailed studies have been performed on the crystal structure of PANI.[7,21] The standard method of crystal structure analysis requires the development of a single crystal of the material, its detailed optical analysis, the determination of the crystal system and unit cell dimension, the measurement of crystal density, the calculation of unit cell content, the hkl recording, and space group determination.[22–25] Therefore, extensive analysis is required to obtain the crystal structure of a molecule. Moreover, it is not always easy to grow a single crystal for all crystalline materials.[21] Although the determination of a crystal structure based on X-ray analysis of a powdered sample is relatively easy, the method has several limitations.[22] Recently, computer simulation of crystal structures has attracted great attention.[20] The Fullprof is one of the widely used software packages for this purpose.[26–28] Available literature concerning the crystal structure analysis of semi-crystalline organic polymers, such as PANI, using different software

Correspondence to: J. H. Lee (jhl@chonbuk.ac.kr).

packages is relatively rare compared with that for a low-molecular inorganic material.[7]

The present research deals with the synthesis of PANI by vapor-phase polymerization and conventional chemical oxidative polymerization of aniline. The PANI obtained by vapor-phase polymerization is designated as PANI-V and the PANI obtained by chemical polymerization is designated as PANI-C. A comparison of their properties is performed through conductivity, solubility, contact angle, Fourier transform infrared (FTIR), UV, thermogravimetric analysis (TGA), and FE-TEM analysis. An in-depth investigation of the crystal structures of PANI-C and PANI-V was performed through a powder X-ray diffraction analysis using FullProf and FOX v. 1.7 OSVN software.

EXPERIMENTAL

Materials

Aniline was obtained from Kanto Chemical, Japan, while ammonium persulfate (APS) and *N*-methyl-2-pyrrolidone (NMP) was purchased from Sigma Aldrich, Germany. Methanol was procured from Samchun Pure Chemicals, Korea, and hydrochloric acid was bought from Duksan Pure Chemicals, Korea. Tetrahydrofuran (THF), *N*,*N*-dimethyl formamide (DMF), dimethylsulfoxide (DMSO), and *m*-cresol were obtained from Tokyo Chemical Industry, Japan. All these chemicals are guaranteed reagents (GR) suitable for use in analytical chemistry. Aniline was distilled before use. Other chemicals were used as received.

Synthesis of polyaniline by conventional oxidative polymerization (PANI-C)

A total of 9.3 ml (0.1 M) of aniline, 2 mL (0.05 M) of concentrated HCl (50 mole % with respect to aniline) and 100 mL distilled water were placed in a beaker, and were stirred for 5 min with a magnetic stirrer for homogenization. A total of 22.8 g (0.1 M) of APS (equimolar amount with respect to aniline) was then dissolved in 10 mL of water. This aqueous solution of APS was then added drop wise into the reaction beaker and the polymerization reaction was performed for 6 h at room temperature (25 $\pm$ 5°C) while being constantly stirred. The molar ratios of monomer (aniline) to oxidant (APS) 1 : 1 and monomer to dopant (HCl) of 1 : 0.5 were chosen because it was found that with these ratios, the productivity and conductivity of the resultant polymer is very good.[3] After 6 h of reaction, the polymerization was stopped through the addition of 50 mL methanol to the reaction mixture. A deep-green PANI was precipitated, which was filtered, thoroughly washed with distilled water to remove unreacted chemicals, and then dried in a vacuum oven at 60°C for 48 h. Finally, the dried PANI powder was recrystallized from methanol and again dried in a vacuum oven at 60°C for 48 h. The PANI produced is designated as PANI-C. The yield of PANI-C was 89.6%.

Synthesis of polyaniline by vapor-phase polymerization (PANI-V)

A total of 9.3 ml of aniline was placed into a round-bottomed (RB) flux. A total of 2 mL of HCl, 22.8 g of APS and 100 mL of deionized water were placed into another RB flux. These two RB fluxes were connected with a hollow glass tube. The RB flux containing aniline was heated at 200°C to generate aniline vapor. The aniline vapor thus produced was inserted through the hollow glass tube into the second RB flux containing the aqueous acidic solution of APS while being constantly stirred. The transparent aqueous acidic APS solution slowly turned into a green-colored solution. The solution was stirred for 6 h to form a well-developed polymer. A green-colored precipitate was formed, which was filtered, thoroughly washed with distilled water to remove unreacted chemicals, and then dried in a vacuum oven at 60°C for 48 h. Finally, the dried PANI powder was recrystallized from methanol and again dried in a vacuum oven at 60°C for 48 h. Thus, the PANI produced is designated as PANI-V. The yield of PANI-V was 66.3%.

Characterization

The DC electrical conductivity was measured under laboratory conditions by the four-point probe method using a programmable DC voltage detector, a 2182-A Nanovoltameter (Kithley, USA) and a 6220 precision current source (Keithley, USA). The sample powder was compacted into a disk pellet with a diameter of 12.6 mm and a thickness of about 0.25 mm by applying a pressure of 10 tons. All data represent the average value of the measurements from at least five samples.

The water contact angle was measured under laboratory conditions using a Phoenix-300, Surface electrooptics, from Korea. The powder was compacted into a disk pellet under a pressure of 10 tons and the contact angle of water on this pellet was then measured.

The FTIR spectra were recorded on a NICOLET 6700 FTIR (Thermoscientific, USA). Samples were dispersed in KBr powder and compressed into pellets. OMNIC software was used for the baseline correction and calculation of the peak area.

The TGA was performed using TGA, Q50, TA Instruments, from USA. The experiment was

performed under a nitrogen atmosphere within a temperature range of 35°C–900°C at the heating rate of 20°C/min.

The UV-visible spectra were recorded at ambient temperature using a UVS-2100 SCINCO spectrophotometer. Stock solutions were prepared by dissolving each sample (0.5 g/L) in THF, NMP, DMF, *m*-cresol, and then filtering them through a 1.0-μm filter unit. The band energy for different absorption bands was calculated from the following equation

$$\Delta E = \frac{hc}{\lambda_{max}} \tag{1}$$

$$h = 6.625 \times 10^{-34}\ \text{J.s}, \quad c = 3 \times 10^{8}\ \text{m/s}$$

where ΔE is the band energy, h the Plank's constant, c the velocity of light, and λ_{max} the wave length of the maximum absorption.

The ultrahigh resolution microscopic study was performed using a field emission transmission electron microscope (FE-TEM), JEM-2200 FS from JEOL, Japan, with an accelerating voltage of 200 keV. The polymer powder was dispersed in ethanol and sonicated for half an hour to break the clusters. One drop of this dispersion was added on the sample grid (copper–carbon), dried, and then used for the experiment. Several images were taken for each sample. The particle size was determined using Image-Pro software from each image and there range of size is reported.

The X-ray diffraction study was performed using D/MAX 2500V/PC, from the Rigaku Corporation, Japan, using a copper target (Cu Kα) forming an X-ray wave length of 1.5418 Å. The data was recorded from $2\theta = 5$–50° (because beyond 50° there was no peak).

The XY (2*theta vs. intensity) data obtained from this experiment was plotted using the WINPLOTR program and the angular position of the peaks was obtained using the sane program.[29] The dimension of the unit cell, hkl values, and space groups of all these polymers were obtained after running the DICVOL program in the FullProf software package. Refinement was then performed through the routine profile matching of FullProf.[30–33] The arrangement of the polymer chains in the unit cell was determined using FOX v. 1.7. OSVN software after substituting the values of unit cell dimensions and the space group obtained from the DICVOL program. The orientation was optimized and the configuration was randomized. The XY (2*theta vs. intensity) was also plotted using Origin 6.1. Smoothing was performed by adjacent averaging methods considering five points. A straight line was then subtracted to obtain $Y = 0$. Finally, a Gaussian fit for multiple peaks was performed to determine the areas of different peaks and their full width at half maxima. The degree of crystallinity (%) was calculated from the ratio of crystalline peak area to total peak area. The d-spacing (D) corresponding to the highest intense crystalline peak was determined by the Debye-Scherrer (powder) method using Bragg's relation.[34,35]

$$n\lambda = 2D \sin\theta \tag{2}$$

where n is an integer, λ the wavelength of the X-ray, which is 1.54 Å for Cu target, and θ the angle between the incident and reflected rays.

The crystallite size (T) corresponding to the highest intense crystalline peak was determined from the Scherrer relation.[36]

$$T = \frac{K\lambda}{B \cos\theta} \tag{3}$$

where K is the shape factor for the average crystallite (~ 0.9), and B the full width at half maxima of the crystalline peak in radians.

The interchain separation length (R) corresponding to the highest intense crystalline peak was determined from the relation given by Klug and Alexander.[37]

$$R = \frac{5\lambda}{8 \sin\theta} \tag{4}$$

RESULTS AND DISCUSSION

The conductivity and water contact angle of PANI-C and PANI-V are presented in Table I. The conductivities of PANI-C and PANI-V are 0.073 and 0.058 S/cm, respectively. PANI has three basic structures based on its oxidation level: (I) a pernigraniline base (PNB), which is fully oxidized and all repeat units have a quinoid structure (Q); (II) a leucoemeraldine base (LEB), which is fully reduced and all repeat units have a benzenoid structure (B); and (III) a half-oxidized emeraldine base (EB) where the Q to B ratio is 1 [Fig. 1(a)]. The doped half-oxidized and half-reduced emeraldine base (EB) first forms a bipolaron [Fig. 1(b)] followed by a polaron [Fig. 1(c)], which is significantly conducting in nature. Conduction in a polaron structure occurs through the hopping of charge carriers. However, LEB and PNB are relatively insulating in nature. Conductivity of doped

TABLE I
Conductivity and Water Contact Angle of PANI-C and PANI-V

Properties	PANI-C	PANI-V
Conductivity (S/cm)	0.073	0.058
Water contact angle (degree)	61.8	52.7

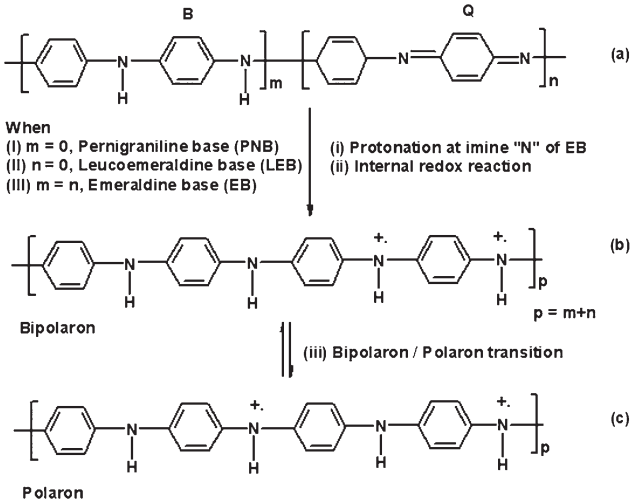

Figure 1 (a) Different structure of PANI based on oxidation level: (I) fully oxidized pernigraniline base (PNB), (II) fully reduced leucoemeraldine base (LEB), and (III) half-oxidized emeraldine base (EB), (b) bipolaron formation after protonation of EB, and (c) bipolaron to polaron transition.

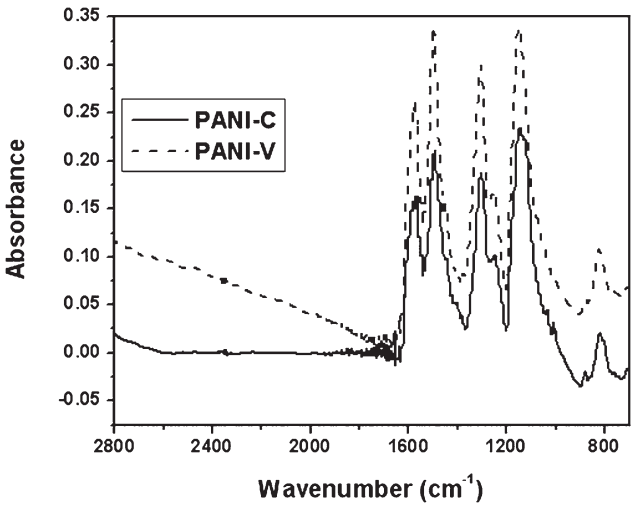

Figure 2 FTIR spectra of PANI-C and PANI-V.

PANI mainly depends on its oxidation level, degree of doping, degree of crystallinity, and interchain separation.[3,4] The synthesized PANI samples are significantly conducting in nature, showing that these PANI samples contain a high concentration of an EB form. The PANI-V shows relatively lower conductivity compared with PANI-C. The water contact angle for PANI-C is 61.8° and that for PANI-V is 52.7°. The lower water contact angle of PANI-V indicates that its water wettability or hydrophilicity is higher than that of PANI-C.[38]

The solubility of PANI-C and PANI-V was measured at room temperature in different solvents, such as THF, NMP, DMSO, DMF, and *m*-cresol as presented in Table II. Each reported solubility is the average of five measurements. The standard deviation of these five values was calculated and presented in Table II. The solubility of PANI-V is two to three times higher than PANI-C in all these solvents. The degrees of solubility for both the polymers are different in different solvents because of the difference in interaction between polymer–solvent. NMP and *m*-cresol are better solvents for PANI than THF, DMSO, and DMF.

TABLE II
Solubility of PANI-C and PANI-V at Room Temperature in Different Solvents with Standard Deviation

Solvent	Solubility of PANI-C (g/L)	Standard deviation	Solubility of PANI-V (g/L)	Standard deviation
THF	0.5	0.04	1.4	0.14
NMP	2.3	0.15	5.8	0.09
DMSO	1.3	0.12	3.2	0.23
DMF	0.8	0.08	1.7	0.12
m-cresol	2.6	0.15	3.8	0.16

The FTIR spectra of PANI-C and PANI-V are shown in Figure 2. PANI-C shows six major absorption peaks. The infrared absorption peaks at 1573 and 1494 cm^{-1} for PANI-C are assigned for the quinoid (Q) and benzenoid (B) ring stretching deformations, respectively.[4,5,39,40] The band at 1301 cm^{-1} is due to the π electron delocalization induced in the polymer through protonation or C—N—C stretching vibration.[39,40] The band at 1246 cm^{-1} is the characteristic of the $C—N^+$ stretching vibration in the polaron structure.[5] The absorption band at 1145 cm^{-1} corresponds to the vibration mode of the $—NH^+=$ in the protonated emeraldine base.[39–41] The band at 820 cm^{-1} represents the C—H out of plane deformation of 1, 4-disubstituted benzene rings.[42] All these six absorption bands at 1573, 1494, 1301, 1246, 1145, and 820 cm^{-1} for PANI-C are blue shifted at 1581, 1498, 1306, 1249, 1150, and 823 cm^{-1}, respectively, for PANI-V. The blue shift of all these bands in PANI-V may be due to the lower degree of protonation.[42] From the ratio of peak areas corresponding to the quinoid (Q) and benzenoid (B) ring stretching deformation, the oxidation level of PANI was determined.[5,39,40,43] The oxidation levels (Q/B) of PANI-C and PANI-V are found to be 0.60 and 0.65, respectively. The higher level of oxidation in PANI-V compared with PANI-C may be due to the easier contact between the monomer and oxidant in the vapor phase than that of the solution or dispersion state. The oxidation level indicates that the PANI-V contains more emeraldine base (EB) forms and hence it should exhibit a higher conductivity.[4,5,39,40,43]

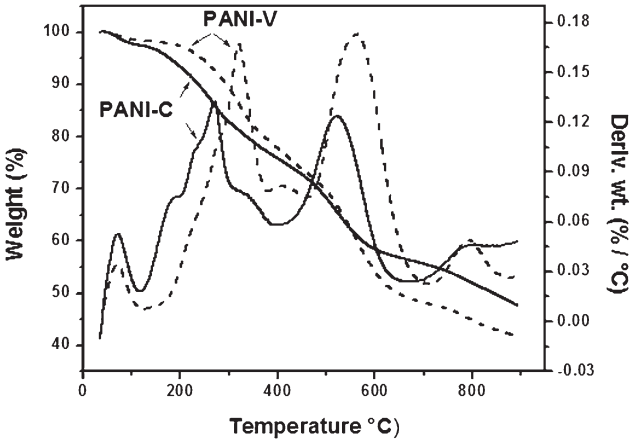

Figure 3 TGA plots of PANI-C and PANI-V.

However, experimentally, it was found that the conductivity of PANI-C is higher than that of PANI-V. This may be due to a higher degree of doping in PANI-C compared with that of PANI-V.

Figure 3 represents the TGA plots of PANI-C and PANI-V. There are four steps of weight loss observed during the heating of the PANI samples under a nitrogen atmosphere. The first step of weight loss observed within the temperature range of 50°C–150°C is due to the loss of moisture. The second step of weight loss occurring between 150°C and 400°C is due to the loss of dopant. The third step of weight loss within 400°C–700°C occurs for the thermal decomposition of PANI into some chemical forms. The final step of weight loss at around 700°C–900°C is due to the final carbonization of intermediate chemicals.[4,5,39,40,43] The decomposition peak temperature for PANI-C and PANI-V are 520°C and 560°C, respectively. This shows that PANI-V is thermally more stable than PANI-C. The weight loss percentage of HCl and PANI are divided by the respective molecular weights of HCl and the monomer unit of PANI to obtain the relative mole percentage of HCl and PANI present in the sample. The mole percentage of HCl is divided by the mole percentage of PANI and multiplied by 100 to obtain the relative mole percentage of HCl in PANI, which is the degree of doping.[4] The degrees of doping of PANI-C and PANI-V are found to be 70% and 60%, respectively.[43] This result is in good agreement with the blue shift for PANI-V in the FTIR spectrum.

The solubility of PANI is very low and it changes with changing solvent. Hence, the UV spectra of PANI-C and PANI-V were taken in different solvents, such as THF [Fig. 4(a)], NMP [Fig. 4(b)], DMF [Fig. 4(c)] and *m*-cresol [Fig. 4(d)]. Three characteristic absorption bands are observed for both polymers in all the solvents, first band at around 250–310 nm, second band at around 310–450 nm, and third band at around 450–800 nm. The first absorption is assigned to the π–π* transition and the second and third absorptions are ascribed to the bipolaron/

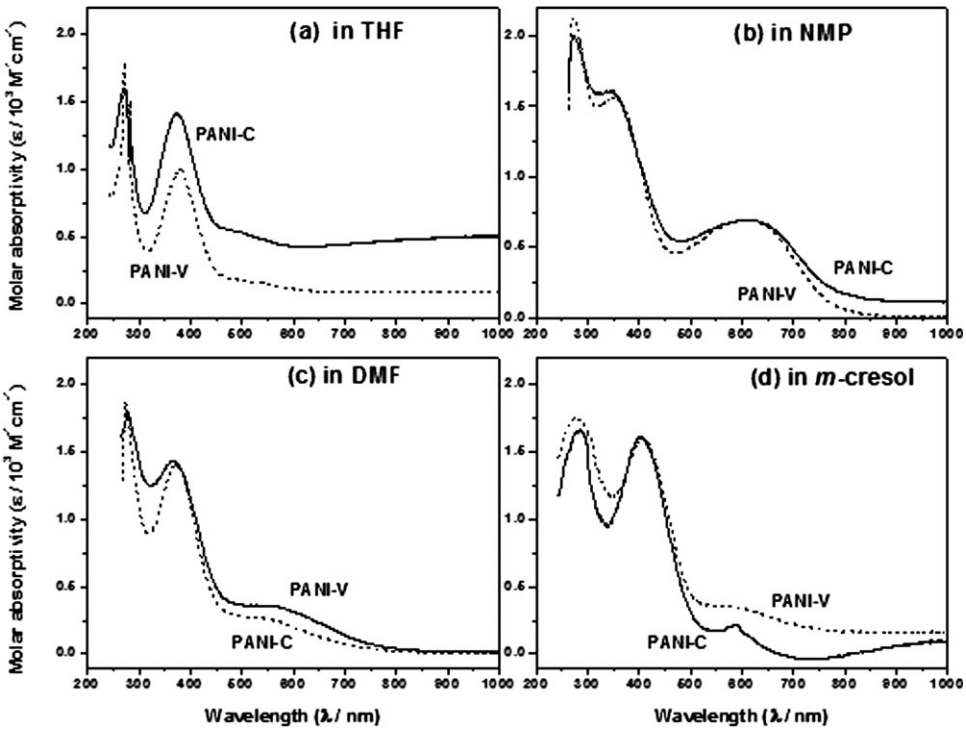

Figure 4 UV-vis spectra of PANI-C and PANI-V in (a) THF, (b) NMP, (c) DMF, and (d) *m*-cresol.

TABLE III
Wavelength of the Maximum Absorption (λmax) and Corresponding Band Energy (Δ*E*) and Maximum Molar Absorptivity (ε_{max}) of PANI-C and PANI-V in Different Solvents

Sample	λ_{max} (nm)	ΔE (eV)	ε_{max} (x 10^3 $M^{-1}cm^{-1}$)
PANI-C in THF	271	4.58	1.60
	374	3.32	1.40
	511	2.43	0.52
PANI-V in THF	270	4.60	1.80
	380	3.27	1.00
	537	2.31	0.16
PANI-C in NMP	274	4.53	1.99
	347	3.58	1.62
	609	2.04	0.70
PANI-V in NMP	271	4.58	2.13
	354	3.51	1.57
	616	2.02	0.70
PANI-C in DMF	280	4.44	1.79
	366	3.39	1.43
	561	2.21	0.35
PANI-V in DMF	274	4.53	1.88
	371	3.35	1.40
	565	2.20	0.25
PANI-C in *m*-cresol	284	4.37	1.67
	402	3.09	1.61
	587	2.12	0.22
PANI-V in *m*-cresol	275	4.52	1.75
	409	3.04	1.59
	589	2.11	0.35

polaron transition [Fig. 1(b–c)] that occurs in the doped PANI.[6,39,40,43] As the possibility of these transitions in PANI increases, the expected conductivity concurrently increases. The nature of the first band is almost similar in all four solvents; however, the pattern of second and third band is different in different solvent. This fact indicates that the effect of solvent is more pronounced for the bipolaron/polaron transition compared with the π–π* transition in PANI. First two bands are very strong in all four solvents, whereas the third band is strong in NMP but weak in THF, DMF, and *m*-cresol. The wavelength of the maximum absorption (λ_{max}), the calculated band energy (ΔE), and the maximum molar absorptivity (ε_{max}) corresponding to each band for PANI-C and PANI-V are presented in Table III. PANI-C shows a marginally higher λ_{max} value but a lower ΔE and ε_{max} values for the π–π* transition (first band) in all solvents. These results indicate that the π–π* transition is easier; whereas the intensity of this transition is little lower in PANI-C. This may be due to the presence of less EB structure in PANI-C than in PANI-V (found from FTIR analysis). The λ_{max} value is lower, whereas the ΔE and ε_{max} values are higher for the bipolaron/polaron transition (second and third band) in PANI-C compared with that of PANI-V. These results demonstrate that the bipolaron/polaron transition is easier in PANI-V due to the presence of more EB forms, yet the intensity of this transition is less (except third band in *m*-cresol) due to a lower degree of protonation in PANI-V compared with that of PANI-C as found from TGA analysis. These results are in sound agreement with the FTIR and TGA results. The wave length of visible light is 400–700 nm and the wave length corresponding to the third absorption band PANI-C and PANI-V in all solvents are within the visible range. However, the λ_{max}, ΔE, and ε_{max} values for third band are widely different in different solvents. PANI interacts differently with different solvent and appears with different color. The region of absorption band for violet, blue, green, yellow, orange, and red colored materials are 400–424, 425–491, 491–575, 575–585, 585–647, and 647–700 nm, respectively.[6,44] Hence, the absorption characteristics of same molecule in different solvent is different in the visible region due to the appearance of different color leading to the variation in λ_{max}, ΔE, and ε_{max} values.

The field emission transmission electron microscopic (FE-TEM) images of PANI-C and PANI-V are shown in Figure 5. Both PANI-C and PANI-V have irregular shape, size, and surface. The length and diameter of PANI-C range from 100 to 2000 nm and 100 to 700 nm, respectively. On the other hand, the length and diameter of PANI-V range from 50 to 400 nm and 20 to 100 nm, respectively. The PANI-V has a much smaller particle size and very narrow particle size distribution compared with PANI-C.

The higher solubility and lower size of PANI-V indicates that the molecular weight of these polymers may be lower than the PANI-C. This may be due to the easier contact between the monomer and oxidant in the vapor phase leading to the growth of higher number of polymer chains with lower length than that of the solution or dispersion state. Therefore, vapor-phase polymerization may prove to be a good route for the preparation of nanostructured polymer.

The X-ray diffraction plots of PANI-C and PANI-V are presented in Figure 6. The plots show few crystalline peaks and few amorphous regions. PANI is a semi-crystalline polymer with a two-phase system. In the crystalline phase polymer, the chains are parallel and orderly arranged, and in the amorphous phase polymer, the chains are not orderly arranged and do not have parallel alignment. The crystalline phase may be of different types depending on the nature of the polymer and can be detected from the X-ray diffraction study. The PANI-C exhibits two main crystalline peaks, whereas the PANI-V exhibits three main crystalline peaks. These two crystalline peaks for the PANI-C are located at $2\theta = 20.4^\circ$, corresponding to the d_{-211} crystal plane and at $2\theta = 25.4^\circ$, corresponding to the d_{211} crystal plane [Fig. 6(a)]. The intensity (peak height) represents the

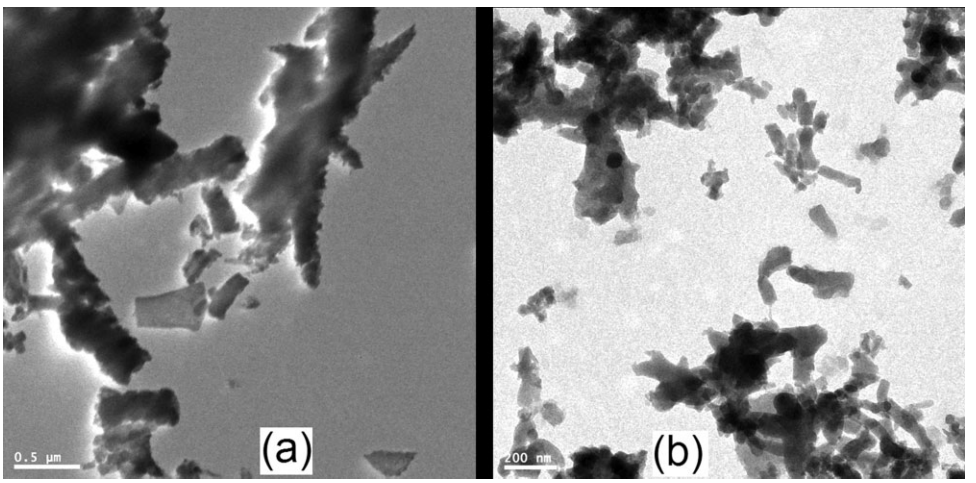

Figure 5 FE-TEM images of (a) PANI-C and (b) PANI-V.

population of crystallite in that plane and the sharpness of the peak represents the degree of regularity or ordered arrangement of polymer chains in the crystallite. The X-ray diffraction pattern of PANI-C indicates that the majority of PANI-C chains are orderly arranged on the d_{211} crystal plane. The main crystalline peaks for PANI-V are located at $2\theta = 6.4^\circ$, 19.2°, and 25.2°, corresponding to d_{010}, d_{030}, and d_{040}, respectively [Fig. 6(b)]. The majority of PANI-V chains are orderly arranged on the d_{030} crystal plane. The main crystalline peaks of PANI-C are sharper than those of PANI-V. From the sharpness of the main crystalline peaks, it can be concluded that the regularity of polymer chains in PANI-C is superior to that of PANI-V.[7]

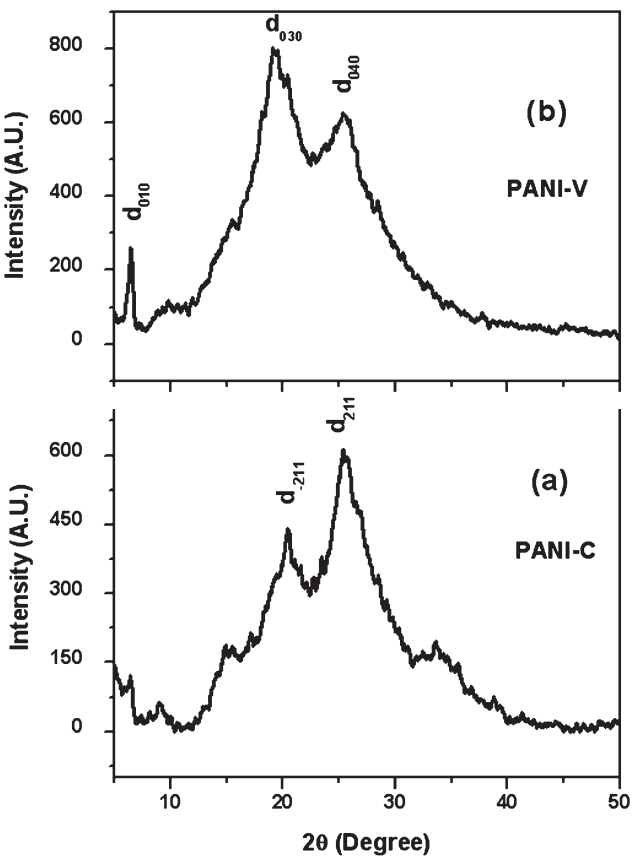

Figure 6 X-ray powder diffraction plots of (a) PANI-C and (b) PANI-V.

The percentage of crystallinity, crystal plane (d_{hkl}), d-spacing (D), interchain separation (R), and crystallite size (*T*) corresponding to the highest intense crystalline peak of PANI-C and PANI-V are presented in Table IV. The crystallinity of PANI-C and PANI-V are 37.3% and 30.2%, respectively. As the degree of regularity in the arrangement and ordering of the polymer chains increases, the crystallinity concurrently increases. The higher crystallinity in PANI-C indicates that the polymer chains in this polymer are more ordered compared with those in PANI-V. This may be due to the difference in their method of synthesis. The d-spacing and interchain separation for PANI-C is much lower than those of

TABLE IV
The Percentage of Crystallinity, Crystal Plane, d-Spacing (D), Interchain Separation I and Crystallite Size (*T*), Corresponding to the Highest Intense Crystalline Peaks of PANI-C and PANI-V

Parameter	PANI-C	PANI-V
Crystallinity (%)	37.3	30.2
Highest intense peak at (2θ/degree)	25.4	19.2
Highest intense crystal plane (d_{hkl})	d_{211}	d_{030}
d-spacing (Å)	3.50	4.61
Interchain separation (Å)	4.38	5.77
Crystallite size (Å)	28.5	22.1

PANI-V. The crystallite size of PANI-C is higher compared with that of PANI-V, which may be due to the higher crystallinity. In PANI, crystalline regions are conducting, whereas amorphous regions are insulating in nature. As the crystallinity in PANI increases, its conductivity is also expected to increase. Again, with the decrease in d-spacing and interchain separation, the probability of interchain hopping is increased leading to the increase in conductivity.[4,39,40,43] The higher conductivity of PANI-C may also be due to its higher crystallinity and lower d-spacing and interchain separation compared with those of PANI-V.

The crystal symmetry, space group, unit cell dimension, and refinement parameters for PANI-C and PANI-V are presented in Table V.

The program and routine profile matching of the FullProf are as follows:

$$R_p = 100\frac{\Sigma|y_i - y_{ci}|}{\Sigma y_i} \tag{5}$$

Here, R_p is the profile factor, y_i the observed intensity, and y_{ci} the calculated intensity at the ith step.

$$R_{\mathrm{wp}} = 100\left[\frac{\Sigma w_i|y_i - y_{ci}|^2}{\Sigma w_i y_i^2}\right]^{1/2} \tag{6}$$

Here, R_{wp} is the weighted profile factor, $w_i = 1/\sigma_i^2$ and σ_i^2 the variance of the observation

$$R_{\mathrm{exp}} = 100\left[\frac{(n-p)}{\Sigma w_i {y_i}^2}\right]^{1/2} \tag{7}$$

TABLE V
Crystal Data and Refinement Factors of PANI-C and PANI-V Obtained After Running the DICVOL Program and Routine Profile Matching of the FullProf

Parameters	PANI-C	PANI-V
Crystal symmetry	Triclinic	Triclinic
Space group	P-1	P-1
a (Å)	8.6764	20.7552
b (Å)	17.3845	19.1921
c (Å)	13.6500	9.8542
α (deg)	25.884	133.116
β (deg)	109.084	136.000
γ (deg)	103.697	63.933
V (Å^3)	840.83	1979.85
R_p	5.88	17.3
R_{wp}	12.7	29.4
R_{exp}	7.27	12.5
R_B	0.576	0.174
R_F	0.671	0.165
χ^2	3.05	5.52
d	0.3648	0.3259
Q_D	1.8049	1.8049
S	1.7	2.3

Here, R_{exp} is the expected weighted profile factor, n and p are the number of profile points and refined parameters, respectively.

$$R_B = 100\frac{\Sigma|I_{\mathrm{obs}} - I_{\mathrm{calc}}|}{\Sigma|I_{\mathrm{obs}}} \tag{8}$$

Here, R_B is the Bragg factor, I_{obs} the observed integrated intensity, and I_{calc} the calculated integrated intensity.

$$R_F = 100\frac{\Sigma|F_{\mathrm{obs}} - F_{\mathrm{calc}}|}{\Sigma|F_{\mathrm{obs}}|} \tag{9}$$

Here, R_F is the crystallographic R_F factor, and F_{obs} is the observed structure factor, $F_{\mathrm{obs}} = \sqrt{(I_{\mathrm{obs}}/L)}$, where L is the Lorentz polarization factor.

$$\chi^2 = \sum w_i(y_i - y_{ci})^2 \tag{10}$$

$$d = \sum \frac{[w_i(y_i - y_{ci}) - w_{i-1}(y_{i-1} - y_{ci-1})]^2}{\sum[w_i(y_i - y_{ci})]^2} \tag{11}$$

Here, d is the Durbin–Watson statistics.

$$Q_D = 2\left[\frac{(n-1)}{(n-p) - \frac{3.0901}{\sqrt{n+2}}}\right] \tag{12}$$

Here, Q_D is the expected Durbin–Watson statistic.

$$S = \frac{R_{\mathrm{wp}}}{R_{\mathrm{exp}}} \tag{13}$$

Here, S is called the goodness of fit.

Both PANI-C and PANI-V have triclinic crystal symmetry and a "P-1" space group. The space group may be described as a set of symmetry elements and it is made up of two parts: a pattern unit and a repeat mechanism. The symbol P represents a primitive unit cell and -1 represents point groups.[23] The unit cell dimensions for PANI-C and PANI-V are different. The unit cell volume of PANI-V is much higher than that of PANI-C.

The Rietveld method involves refining a crystal structure by minimizing the weighted-squared difference between the observed and calculated patterns. A set of conventional factors known as R factors are used to predict the quality of agreement between the observed and calculated profiles. Although commonly used, R_p and R_{wp} agreement factors are not satisfactory from a statistical point of view. A number of statistically more significant parameters, such as d, Q_D, S are also calculated by FullProf. The most common situation in profile refinement is $d < Q_D$, which indicates a positive serial correlation, where successive values of the residuals tend to have the same sign. If $Q_D < d < 4 -$

Q_D, then there is no correlation. If $d > 4 - Q_D$, then there is a negative serial correlation (successive values of the residuals tend to have the opposite signs).[33] For PANI-C and PANI-V, $d < Q_D$, indicating that there is a positive serial correlation between the observed and calculated profiles. The goodness of fit (S) for PANI-C and PANI-V are 1.7 and 2.3, respectively. The goodness of fit for PANI-C is superior to that of PANI-V because as the value of S approaches closer to 1, there is an improvement in the agreement between observed and calculated profiles.

The arrangements of the PANI-C and PANI-V chains in the unit cell are presented in Figures 7 and 8. The PANI-V has a more symmetric unit cell than that of PANI-C. In PANI-C, all carbon and nitrogen atoms are arranged along the direction of the crystal planes and all benzene rings are on the same plane (Fig. 7). In the case of PANI-V, benzene rings and main chain nitrogen atoms are arranged along the direction of crystal planes (Fig. 8). However, not all of the benzene rings are on the same plane. A number of benzene rings have created a disordered region. PANI-C chains are more ordered compared with those of PANI-V. The degree of crystallinity is in good agreement with the arrangement of the polymer chains in the unit cell. The number of atoms in the unit cell of PANI-V is greater due to the higher unit cell volume compared with that of PANI-C.

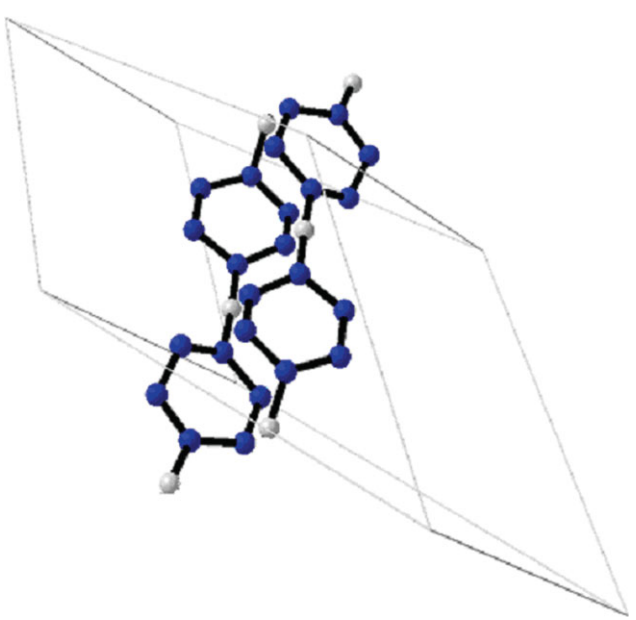

Figure 7 Arrangement of the PANI-C chains in unit cell. [Color figure can be viewed in the online issue, which is available at www.interscience.wiley.com.]

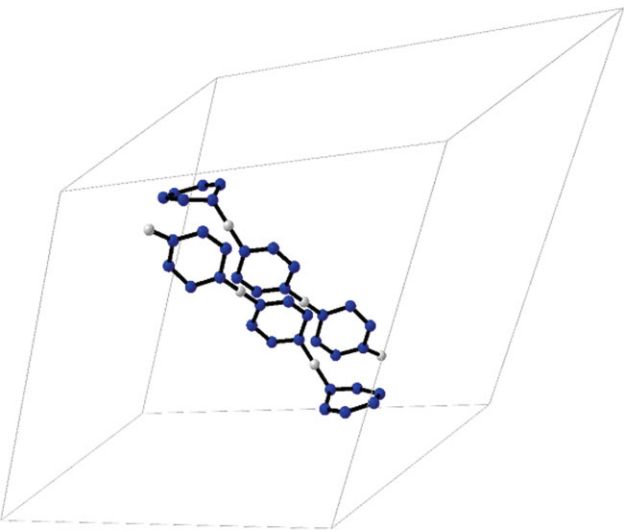

Figure 8 Arrangement of the PANI-V chains in unit cell. [Color figure can be viewed in the online issue, which is available at www.interscience.wiley.com.]

CONCLUSIONS

The polyaniline obtained by the vapor-phase polymerization (PANI-V) shows lower conductivity, higher solubility (two to three times) in different solvents, such as THF, NMP, DMSO, DMF, and *m*-cresol, at room temperature compared with that of conventionally synthesized polyaniline (PANI-C). NMP and *m*-cresol are better solvent than THF, DMSO, and DMF for PANI. PANI-V is more hydrophilic in nature than PANI-C. The higher conductivity of PANI-C may be due to its higher crystallinity, higher degree of doping, lower d-spacing, and lower interchain separation compared with PANI-V. The thermal stability of PANI-V is found to be higher than that of PANI-C. The PANI-C has a more ordered structure compared with the PANI-V. Nanostructured polyaniline with diameter 20–100 nm was obtained from the vapor-phase polymerization. The unit cell volume of PANI-V is much higher, resulting in an increased number of atoms in the unit cell than that of PANI-C. The PANI-V has a more symmetric unit cell than that of PANI-C. Both the polymers show a positive serial correlation between observed and calculated profiles. The goodness of fit for PANI-C and PANI-V are 1.7 and 2.3, respectively.

This study was supported by the National Space Lab (NSL) program (S1 08A01003210) and the 2nd phase BK-21 program funded by the Ministry of Education, Science and Technology, South Korea.

References

1. Angelopoulos, M. IBM J Res Dev 2001, 45, 57.
2. Gospodinova, N.; Terlemezyan, L. Prog Polym Sci 1998, 23, 1443.

3. Bhadra, S.; Singha, N. K.; Khastgir, D. Synth Met 2006, 156, 1148.
4. Bhadra, S.; Chattopadhyay, S.; Singha, N. K.; Khastgir, D. J Polym Sci Part B: Polym Phys 2007, 45, 2046.
5. Bhadra, S.; Khastgir, D. Polym Degrad Stab 2008, 93, 1094.
6. Bhadra, S.; Singha, N. K.; Khastgir, D. Eur Polym J 2008, 44, 1763.
7. Bhadra, S.; Khastgir, D. Polym Test 2008, 27, 851.
8. Erdem, E.; Karakisla, M.; Sacak, M. Eur Polym J 2004, 40, 785.
9. Falcou, A.; Duchene, A.; Hourquebie, P.; Marsacq, D.; Balland-Longeau, A. Synth Met 2005, 149, 115.
10. Li, S.; Dong, H.; Cao, Y. Synth Met 1989, 29, 329.
11. Bissessur, R.; White, W. Mater Chem Phys 2006, 99, 214.
12. Lieber, C. M. Solid State Commun 1998, 107, 607.
13. Zhang, D.; Wang, Y. Mater Sci Eng B 2006, 134, 9.
14. Macdiamid, A. G. Synth Met 2002, 125, 11.
15. Wu, C. G.; Bein, T. Science 1994, 266, 1757.
16. Wan, M. X.; Li, J. J Polym Sci A: Polym Chem 2000, 38, 2359.
17. Park, M. C.; Sun, Q.; Deng, Y. Macromol Rapid Commun 2007, 28, 1237.
18. Chiou, N. R.; Epstein, A. J. Adv Mater 2005, 17, 1679.
19. Zhang, X. Y.; Goux, W. J.; Manohar, S. K. J Am Chem Soc 2004, 126, 4502.
20. Tedesco, E.; Giron, D.; Pfeffer, S. Cryst Eng Comm 2002, 4, 393.
21. Nicolau, Y. F.; Djurado, D. Synth Met 1993, 55, 394.
22. Hageman, J. A.; Wehrens, R.; Gelder, R. D.; Buydens, L. M. C. J Comput Chem 2003, 24, 1043.
23. Ladd, M. F. C.; Palmer, R. A.Structure Determination by X-ray Crystallography; lenum Press: New York, 1988; p 75.
24. Flandorfer, H.; Richter, K. W.; Giester, G.; Ipser, H. J Solid State Chem 2002, 164, 110.
25. Bubnova, R. S.; Krivovichevb, S. V.; Filatov, S. K.; Egorysheva, A. V.; Kargin, Y. F. J Solid State Chem 2007, 180, 596.
26. Sosnowska, I.; Przenioslo, R.; Schafer, W.; Kockelmann, W.; Hempelmann, R.; Wysocki, K. J Alloys Compd 2001, 328, 226.
27. Fernandez, S.; Mesa, J. L.; Pizarro, J. L.; Lezama, L.; Arriortua, M. I.; Rojo, T. Chem Mater 2002, 14, 2300.
28. Rodriguez-Carvajal, J.; Roisnel, T. Mater Sci Forum 2004, 443, 123.
29. Roisnel, J.; Rodriguez-Carvajal, J. WINPLOTR; Laboratoire Leon Brillouin (CEA-CNRS) Centre d'Etudes de Saclay: Gif sur Yvette Cedex, France, 2000.
30. Boultif, A.; Louer, D. J Appl Cryst 2004, 37, 724.
31. Louer, D.; Louer, M. J Appl Cryst 1972, 5, 271.
32. Boultif, A.; Louer, D. J Appl Cryst 1991, 24, 987.
33. Rodriguez-Carvajal, J. An introduction to the program Full-Prof 2000, version July 2001.
34. Castellan, G. W.Physical Chemistry; Narosa publishing house: New Delhi,India, 1996; p 701.
35. Han, D.; Chu, Y.; Yang, L.; Liu, Y.; Lv, Z. Colloids Surf A 2005, 259, 179.
36. Kennedy, C. J.; Lerber, K. V.; Wess, T. J e-Preserv Sci 2005, 2, 31.
37. Klug, H. P.; Alexander, L. E. X-ray Diffraction Procedures; Wiley-Interscience: New York, 1974.
38. Li, Z. F.; Ruckenstein, E. J Colloid Interf Sci 2004, 269, 62.
39. Bhadra, S.; Singha, N. K.; Khastgir, D. J Appl Polym Sci 2007, 104, 1900.
40. Bhadra, S.; Singha, N. K.; Khastgir, D. Polym Int 2007, 56, 919.
41. Chiang, J. C.; Macdiarmid, A. G. Synth Met 1986, 13, 193.
42. Trchova, M.; Sedenkova, I.; Tobolkova, E.; Stejskal, J. Polym Degrad Stab 2004, 86, 179.
43. Bhadra, S.; Chattopadhyay, S.; Singha, N. K.; Khastgir, D. J Appl Polym Sci 2008, 108, 57.
44. Ghosh, S. K.Advanced General Organic Chemistry; Books and Allied (P) Ltd.: Calcutta, India, 1998; p 377.